Parametrical study of the dispersion of an alternative fire suppression agent through a real-size extinguisher system nozzle under realistic aircraft cargo cabin conditions

Raul Payri[a], Jaime Gimeno[a], Pedro Martí-Aldaraví[a,*], César Carvallo[a]

[a] *CMT - Motores Térmicos, Universitat Politècnica de València, Edificio 6D, 46022, Valencia, Spain.*

Abstract

Nearly all active fire extinguishing systems consist of injecting an agent into the space set on fire. For aircraft cargo cabins, the agent widely used up to date is Halon 1301. The FAA provides a level of safety for this fire suppression agent that needs to be used in a volumetric concentration of 6% and needs to be acting for a duration of 0.5 seconds. On the other hand, Halon 1301 is known to contribute to the retrenchment of Earth's atmospheric ozone layer, therefore it is going to be prohibited in the incoming years. The FAA has defined an equivalent level of safety in terms of the performance of the alternative agents. In this research, two different alternative fire suppression agents and two nozzles were tested at two vessel back-pressure conditions using a new design in purpose facility and an injection system able to control the injection pressure and the injection duration (the agent injected mass) in order to satisfy the FAA performance conditions. The discharge volume is a rectangular constant volume constant pressure vessel of approximately 0.85 m^3 and 1.5 m of length that is provided with two transparent windows of 0.75 m x 1.5 m to ensure an optical access to study the whole agent injection and it mixing process. Liquid phase distribution of the agent injected inside the vessel is measured by means of Diffuse Back-Light Illumination (DBI) technique. Vapor phase distribution, when

*Corresponding author. E-mail address: pedmar15@mot.upv.es

R. Payri et al. "Parametrical study of the dispersion of an alternative fire suppression agent through a real-size extinguisher system nozzle under realistic aircraft cargo cabin conditions", Process Safety and Environmental Protection, 141, pp. 110-2122, 2020. DOI: 10.1016/j.psep.2020.04.022

present, is measured through the single-pass Schlieren technique. Results show a poor performance in terms of spatial distribution (narrow jet with little atomization) of the two alternative agents injected through the nozzle actually used in the aircraft cargo cabin fire suppression systems. However, simply replacing the nozzle and using one with a swirler showed excellent performance in terms of spray penetration and spreading angle. This results ratify that the nozzles of the fire extinguisher system currently used in the aircraft cargo cabin does not work for the alternative agents tested.

Keywords: Fire suppression agent, spray, penetration, spreading angle, spatial distribution.

1. Introduction

Fire suppression systems are a requirement for every assembly and construction, also on airplanes [1]. Halon 1301 has long been the choice for fire extinguishment systems for several years, however, due to its high ozone depletion potential its production was banned since 1994 under the Copenhagen Amendments to the Montreal Protocol on Substances that deplete the ozone layer [2] and all the efforts are focused on finding a replacement that yields the same results on fire control in enclosed spaces. In this study, Novec 1230 (dodecafluoro-2-methylpentan-3-one [3]) was used as a possible candidate, in addition to water, fluid widely studied in the literature which reports high efficiency and versatility as a fire extinguishing agent [4]. The present investigation focuses on the analysis of the suppressant distribution into the aircraft cargo cabin volume where fire could occur.

As said by Hipsher and Ferguson [5] the actual technology of smoke detection systems on airplanes can provide an indication of fire in a shorter time within one minute from fire occurs. In all cases, the smoke detection systems can detect a fire at a temperature significantly below that at which the structural integrity of the airplane could be adversely affected.

Halon 1301, once injected through the fire extinguisher system, rapidly evaporates and distributes in the volume due to its low vapor pressure and low boiling point. A concentration of only 7% by volume in air extinguishes fires by a combination of cooling and interference with the chemical reaction chain of fuel and oxygen [6]. For Novec 1230, the required concentration for extinguishment is slightly lower for class B and surface class A hazards (4.5% and 4.1%, respectively) [7]. It has a lower vapor pressure than Halon 1301 but a higher boiling point. The use of water mist as a halon alternative in aircraft cargo compartments was documented and studied by the Federal Aviation Administration [8]. The objective of the water mist fire suppression system in the cargo cabin is to provide a period of protection that will allow the airplane to be landed safely.

The use of high-pressure water mist for extinguishing fires in enclosed spaces has been extensively studied and documented over the years [[9],[10], [11], [12]] due to its advantages such as non-toxicity, non-environmental risk, high efficiency and great utility to face different types and conditions of fire [13]. For fires in enclosed spaces low momentum sprays can be used and the spray flow density required to extinguish them is ten times less than the required to suppress a fire in a well ventilated space of the same size [14]. Chuka et al. [15] studied the effects of droplet size and the orientation of the mist spray injection in the extinction of pool fires and they determined that smaller droplets are much more effective [[16], [17]]. Liu Yinshui et al. [18] studied the effects of the flow rate and the spray cone angle in the water mist fire suppression performance and they concluded that the coverage area of nozzles increased with the angle, while the velocity behaved to the contrary and for fires in an enclosure, the fire extinguishing time increased with the spray cone angle and decreased with the increase in supply pressure and the flow rate. As said by Liang et al.[19] water mist has been studied for decades and it is reliability as a fire extinguishing agent is debated especially for small fires due to it is extinguishing times. For water mist fire suppression systems, an appropriate duration of water supply for each project needs to be selected according to the required time to avoid the re-ignition of small flames that can be present in the area where fire occurs.

Differences in liquid and vapor distributions of these two alternative agents (water and Novec 1230) in a controlled injection event are analyzed for different back-pressure and temperature conditions using two different nozzles. Diffuse Back-light Illumination (DBI) technique is used for visualizing the liquid phase, and single-pass Schlieren for the vapor. The combination of these two techniques allows a better understanding of the injection system and how the condensed-phase is distributed. It may help to propose variations in the actual cargo cabin aircraft extinguisher system, particularly the nozzle.

Nomenclature

Δp	Pressure drop [Pa]	D	Orifice diameter [m]
$\dot{m}$	Mass flow rate [Kg/s]	L	Orifice length [m]
ρ	Density of the fuel [Kg/m^3]	p	Pressure [Pa]
p_{inj}	Injection pressure [Pa]	SOI	Start of injection [s]
A	Area [m^2]	t	Time [s]

2. Materials and Methods

2.1. Test rig, matrix and fluids

The fire extinguishing system used in airplanes consist in a bottle where the working fluid is stored and a nozzle through the fluid is injected [6]. A real cargo cabin fire extinguishing system similar to the one present in the A310 passenger airplane was used as a reference. In order to simplify the experimental measurements, a simple mono-orifice nozzle with an outlet diameter of 2 mm was used. This nozzle was intended for the injection of Halon 1301. Because of this, a poor performance was detected in the injection of Novec 1230 so a new nozzle of Spraying Systems Co Ref 1/4GG-SS3009 with the same outlet diameter and swirler was selected in order to add a tangential component to the flow and improve spray atomization and increase cone spray angle. The

mass flow rate for this new nozzle was to be the same that the old nozzle [20] in order to accomplish the regulations and concentration in volume needed in a fire extinguishing system [7]. In Figure 1 both nozzles used in the experiments can be observed and Table 1 shows the main characteristics of the nozzles.

(a) OldNozzle.

(b) NewNozzle.

Figure 1: Nozzles used in the experimental campaign.

Table 1: Nozzles characteristics.

	OldNozzle	**NewNozzle**
Orifice diameter [mm]	2	2
L/D	0.5	-
Swirler	No	Yes
Max. operating pressure [MPa]	5	2

Figure 2 shows a diagram of the experimental setup used to pressurize and control the injections. The system consists of a pressurized nitrogen bottle of 20 MPa which allows to regulate the system injection pressure, connected to a piston accumulator where the fluid to be injected is stored. The 12 mm diameter line that connects the nozzle with the tank has two solenoid valves (one normally open and one normally closed) responsible for controlling the duration of the injection. The system has pressure and temperature sensors to monitor the injection process. The signal provided by the pressure sensor Kistler 4260A3K0B2FD00Y1 located just before the nozzle was used to obtain the mass flow rate and the total injected mass.

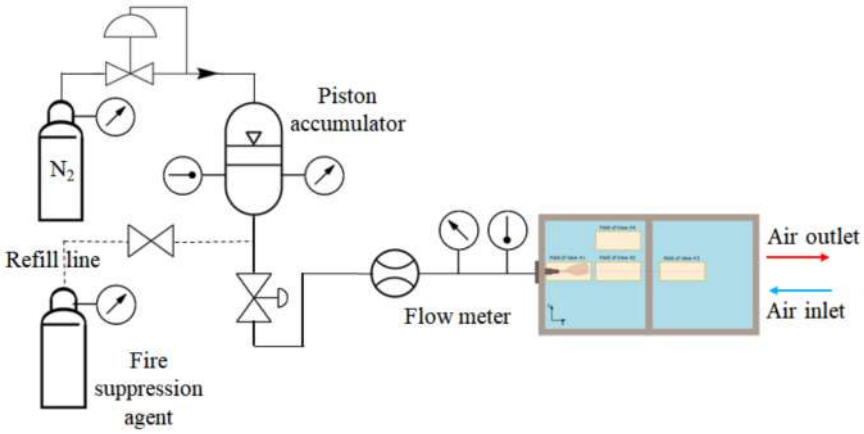

Figure 2: Diagram of injection system.

A picture of the test rig is shown in Figure 3. It is composed of a rectangular sealed prism with an interior volume of $750 \times 750 \times 1500$ mm enough to avoid the spray colliding with the walls during the injection event. The lateral sides of the test rig vessel consists of two transparent windows (750×1500 mm in size and 19 mm thick to withstand the pressure loads).

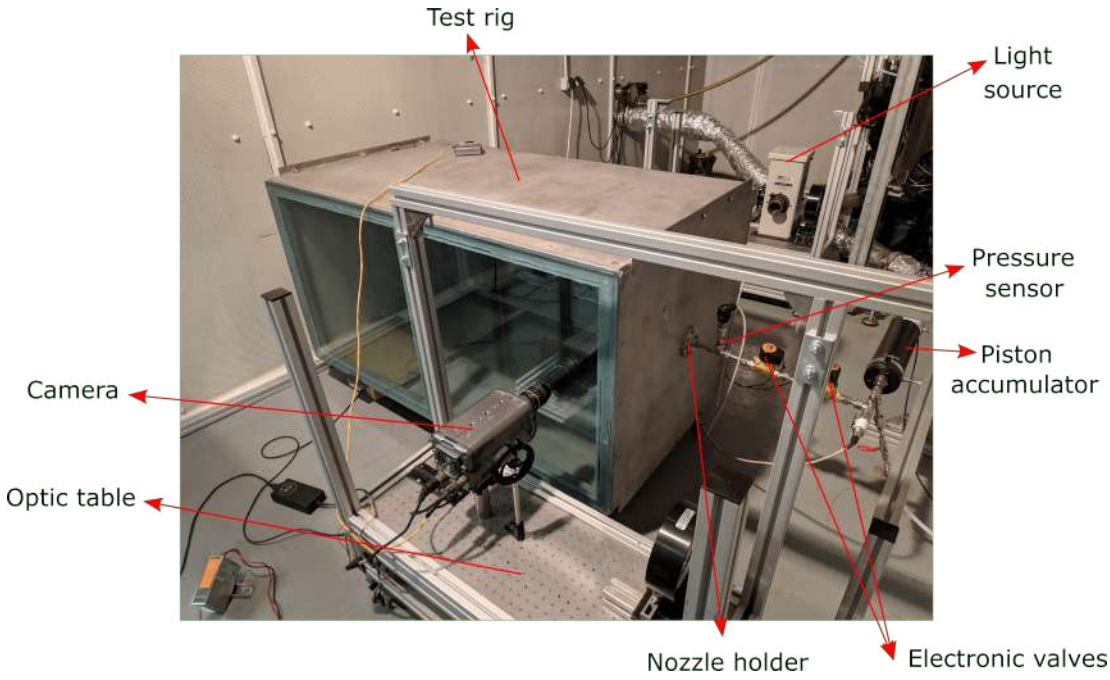

Figure 3: Test rig vessel with DBI optical technique setup.

An air recirculation system was used to renovate the air inside the vessel after each injection event in order to avoid rising in the density of the air because the vapor phase of the Novec 1230 is heavier than the air (can increase up to 7 times the density if the saturated mixture of air and Novec 1230 is reached). The tests were carried out at atmospheric pressure and at 0.75 bar (pressure of the cargo cabin during the flight). In order to reach the low pressure condition inside the test rig a vacuum pump was used.

Preliminary analysis has shown that even with short injection duration, the sprays coming out from the extinguishing system may easily reach more than 1 m in length. Therefore it was necessary to establish different fields of view to study the phenomenon in segments and subsequently analyze the development of the spray as a whole. The visualization windows were limited by the optical elements and by the space of the entire setup (needed to fit inside the climatic chamber). In order to achieve the low temperature conditions the climatic

chamber facility was used for the entire experimental campaign. A diagram of the fields of view (FoV) used to characterize the spray can be seen in Figure 4.

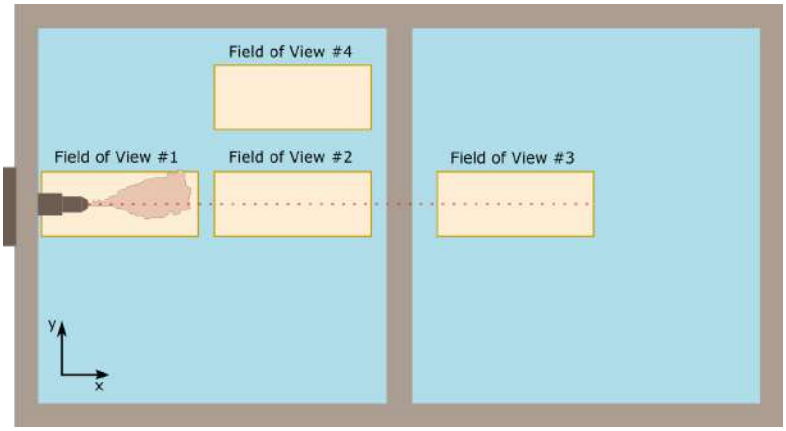

Figure 4: Schematic diagram of the side view of the vessel.

Table 2 shows the exact values of the positions of the fields of view aligned with the axis of the nozzle, except for the field of view #4 which is located above the axis of the nozzle (the FoV #4 overlaps with the FoV #2 but it can not be seen in the figure) to confirm that the spray cone angle obtained in the field of view #1 is maintained throughout the injection event.

Table 2: Position and size of the fields of view.

		Position x-y [mm]	**Width [mm]**	**Height[mm]**
DBI	FoV #1	-11 - 0	171	85
	FoV #2	450 - 0		
	FoV #3	790 - 0		
	FoV #4	450 - 80		
Schlieren	FoV #1	-30 - 0	160	80
	FoV #2	450 - 0		
	FoV #3	790 - 0		
	FoV #4	450 - 80		

Halon 1301 can be stored in small volume as liquid at room temperature

and pressures above 1.61 MPa [21]. The U.S Army has adopted a standard storage of 5.2 MPa at 293 K[6]. In order to reach the actual injection pressures into the aircraft's cargo cabin, losses along the real pipeline system must be taken into account. Those are difficult to estimate and depend on the particular arrangement of each aircraft. Thus, two representative values of the real conditions,1.5 MPa and 2.5 MPa, are selected. However, after completing the entire original test matrix, injections were made with the fluid at low temperature (278 K) and the indoor air temperature of the vessel at 278 K to observe the effects of temperature on the spray development.

The two fluids used as possible fire suppressants were water and Novec 1230. Its thermo-physical properties [[22]] are compared with Halon 1301 [6] in Table 3. These properties play a fundamental role in the development of the spray, widely discussed by Reitz et al. [23]. and this will be shown later in this work.

Table 3: Thermo-physical properties of Halon 1301 and the alternative suppressants. All values at 298 K unless otherwise specified.

Property	**Halon 1301**	**Water**	**Novec 1230**
Chemical formula	CF_3Br	H_2O	$CF_3CF_2C(O)CF(CF_3)_2$
Molecular weight[g/mol)]	148.91	18.02	316.04
Boiling point at 0.1 MPa [K]	215.35	373.15	322.25
Freezing point [K]	105.15	273.15	165.15
Vapor pressure [MPa]	1.47	0.04	0.002
Density [kg/m^3]	1551	1000	1616
Liquid viscosity [kg/ms]	0.16e-3	1.03e-3	0.39e-3
Surface tension [N/m]	5.95e-3	72.75e-3	108e-3

2.2. Diffuse back-illumination imaging(DBI)

Diffuse back-illumination imaging (DBI) is one of the established measurement techniques applied by the Energy Combustion Network (ECN) for liquid phase penetration [24]. It consists in the determination of the shape of the spray liquid phase based on the silhouette obtained by the obstruction of a beam of diffuse light with the spray at inert conditions. The setup utilized for

this method is represented in Figure 5. The light beam is produced by a high power continuous light source and goes through a diffuser which homogenizes and smooths the background of the spray image. After trespassing the measurement section, the light goes to a high-speed Phantom V12 camera that records the spray injection. An example of the images recorded using this technique in all fields of view of Table 2 is shown in Figure 6.

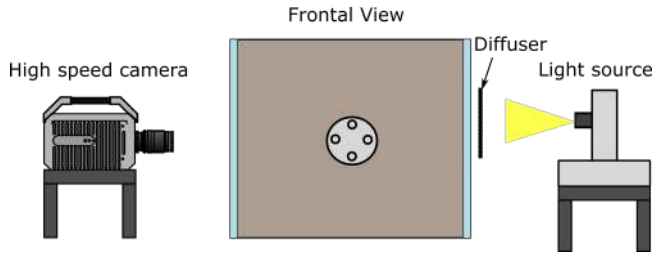

Figure 5: Scheme of the DBI optical setup.

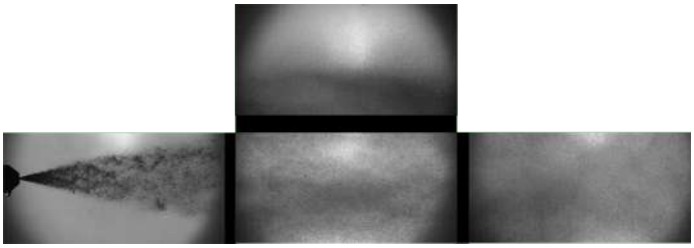

(a) Water at 2.5 MPa and back-pressure of 0.1 MPa with DBI optical technique.

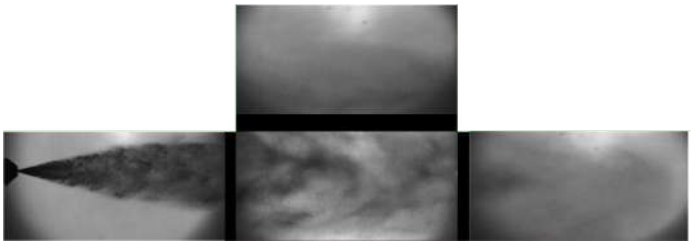

(b) Novec at 2.5 MPa and back-pressure of 0.1 MPa with DBI optical technique.

Figure 6: Example of the images acquired with DBI technique for all the field of views.

2.3. Schlieren single-pass

Schlieren imaging technique is based on the fact that light rays are deflected as a consequence of them trespassing through a medium with density changes [25]. It consists of a beam of parallel rays that travels through the section where the fluid is injected and filtering or discarding some of the deflected light allows to extract information of the spray, such vapor penetration and vapor phase spray cone angle. To detect the spray boundaries, a conventional Schlieren single-pass setup is employed, whose scheme is shown in Figure 7. This configuration is meticulously described by Pastor et al. [26]. A punctual light source was placed at the focal length from a lens. The incident angle between the source and the lens was minimized in order to reduce the beam straightening. After the lens, the now parallel light beams are directed across the testing region obtaining, as a result of the deviation of light, information about the spray development inside the vessel. This deviated beams are collected by another lens with a 450 mm focal distance which collects the light coming from the testing zone and focuses in a point where a diaphragm (also known as plane of Fourier[26]) was located with a cut-off diameter of 5 mm just before the high-speed camera. As before, an example of the images recorded using this technique is shown in Figure 8. The Schlieren technique was not used for water because for this fluid the spray did not evaporate under the injection conditions tested [20].

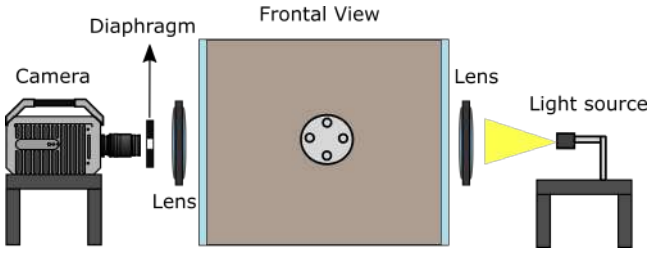

Figure 7: Scheme of the Schlieren optical setup.

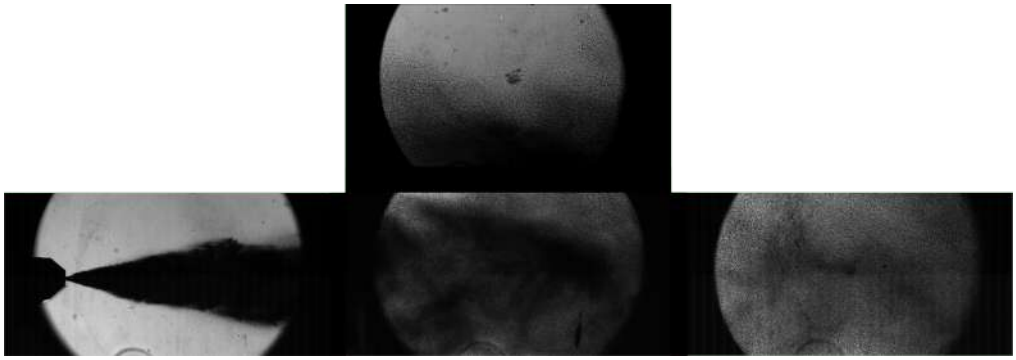

Figure 8: Example of the images acquired with the Schlieren technique for Novec 1230 at 2.5 MPa and back pressure of 0.1 Mpa for all the field of views.

2.4. Image processing

The image processing methodologies are based on strategies to segment the spray and background. The core of the segmentation algorithm is based in a fixed threshold intensity-sensitive method [[27],[28],[29],[30],[31]].

The principle behind the fixed threshold method is the binarization of the image with an intensity level, usually calculated as a constant percentage (or fixed threshold) of the dynamic range of a frame. This procedure is used for optical techniques like Mie scattering, Schlieren or diffused back illumination. The most difficult task is to achieve a proper background subtraction, especially in Schlieren, as it presents pixel structures of the same intensity level as the spray. The thresholds used were 0.04 for DBI and 0.08 for Schlieren. In order to obtain the macroscopic spray parameters of penetration in both, liquid and vapor phases and the spray cone angle from the images recorded the following methodology was used:

- Background correction

  In order to remove reflections and objects that could generate bad estimations of the contour, the background is taken as the image acquired before the start of injection, and is subtracted arithmetically.

- Spray boundaries detection

Employing the approach used by Siebers in [32], the contour was calculated binarizing the image. In Figure 9 the image series shows the typical spray boundary detection routine while it is penetrating across the chamber. To mitigate the noise effect related to the image and to ensure a robust detection of the liquid phase silhouette, the threshold of the intensity is changed to guarantee a correct boundary detection of the spray.

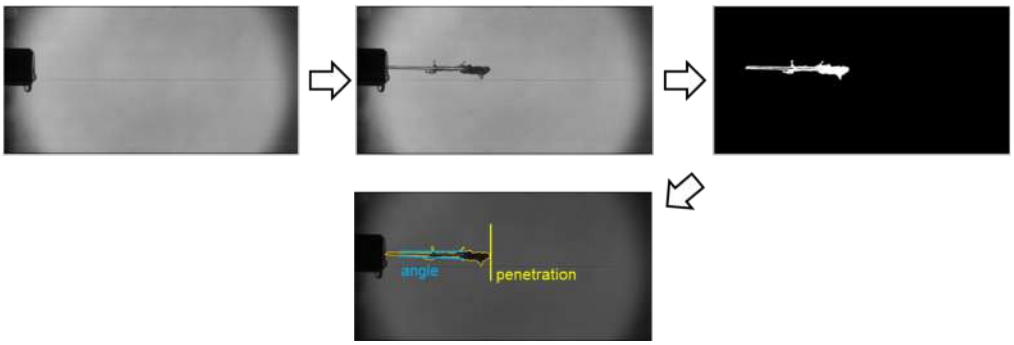

Figure 9: Steps of the image processing routine.

– Contour analysis

  Once the contour of the spray has been obtained, it is possible to calculate some of their geometrical features. Of these characteristics, those related to this work are the penetrations for both, the liquid and the vapor phase that are calculated as the furthest position of the spray contour in the images obtained by DBI or Schlieren imaging.

– Spreading angle

  Once penetration has been calculated, the spray cone angle is estimated as the angle of the trapezium whose bases are the segments inside the contour that coincide with distances of 12% and 50% of the instantaneous penetration from the tip of the injector.

The four different fields of view were not recorded simultaneously. In other words, each repetition of each field of view corresponds to a different injection

event. The acquired pressure signal on the pipe just upstream the nozzles is used to define the start of injection (SOI) and synchronize all repetitions and fields of views of the same injection conditions. Up to 5 repetitions of each test point and field of view were performed, acquired and processed.

2.5. Test matrix

Including a new nozzle, back pressure of 0.075 MPa to reproduce the real aircraft cargo cabin conditions and variations in the temperature for the air inside the test rig vessel and the injected fluid. Table 4 shows the conditions tested, only two fields of view in low temperature conditions (278 K).

The test matrix was used for both fluid and it includes conditions in which the fire can occur, both on the ground at sea level as in the air with conditions equivalent to 2500 m above the sea level. Tests with low temperature conditions for water (278 K) were not carried out due to the freezing risk that could occur inside the injection pipe since the cooling system used in the experiments had a temperature offset of 10 K.

Table 4: Complete test matrix.

Injection pressure [MPa]	**Ambient gas pressure** [MPa]	**Ambient gas temperature** [K]	**Fluid temperature** [K]	**Injection duration** [s]	**Field of view** -
1.5	0.075	298	298	0.05	All
1.5	0.075	278	278	0.05	1-2
1.5	0.1	298	298	0.05	All
1.5	0.1	278	278	0.05	1-2
2.5	0.075	298	298	0.05	All
2.5	0.075	278	278	0.05	1-2
2.5	0.1	298	298	0.05	All
2.5	0.1	278	278	0.05	1-2

3. Results and discussion

3.1. Rate of injection

For the ILASS 2019 congress, the discharge coefficient was estimated for simple geometry nozzles [33] because the discharge of an incompressible non-cavitating fluid through an orifice can be written in the form of Equation 1. In that case of study with the factor L/D = 0.5 and the corresponding Reynolds a $C_d = 0.64$ was obtained. Instead, the discharge coefficient for the new nozzle with swirler is obtained by multiple injections and the injected mass measured in a gravimetric balance to check if the injected mass for both nozzles is the same and able to satisfy the requirements of a fire extinguishing system. Subsequently, the discharge coefficient obtained ($C_d = 0.76$) resulted similar to the one provided by the manufacturer. The injected mass comparison can be seen in Figure 10

$$C_d = \frac{\dot{m}}{A\sqrt{2\rho\Delta p}} \tag{1}$$

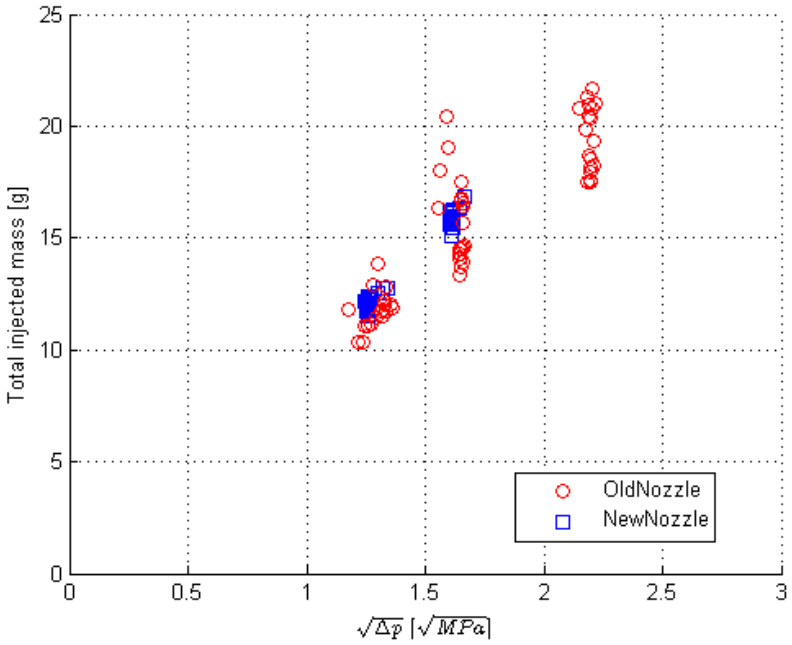

Figure 10: Injected mass comparison between nozzles.

Figure 11 shows the mass flow rate curves calculated for all the conditions described in Table 4 for the NewNozzle due to the results are equivalents for both nozzles. The standard deviation of the average mass flow curves, taken in the steady state zone of the injection event, vary between 2% and 5%. Temperature and pressure play a fundamental role in the process of evaporation of the injected fluid. There is a clear trend for Novec1230 that differentiate the condition of low chamber back-pressure (dashed lines) with the ones at ambient pressure (solid lines) at 298 K of temperature because the remaining Novec1230 in the pipe evaporates producing the unstable behavior saw at the beginning of the injection process. The curves corresponding to the low temperature injections do not show a drastic change between the two chamber back pressures since the evaporation phenomenon is weaker.

As expected due to its higher density, the Novec1230 mass flow rate is higher and also, higher the injection pressure higher the mass flow rate.

In the case of water Figure 11.e), back-pressure changes at 298 K did not produce significant differences in the mass flow rate curves due to the water volatility produced by its higher vapor pressure is lesser than Novec1230 and does not evaporate easily under these injection conditions.

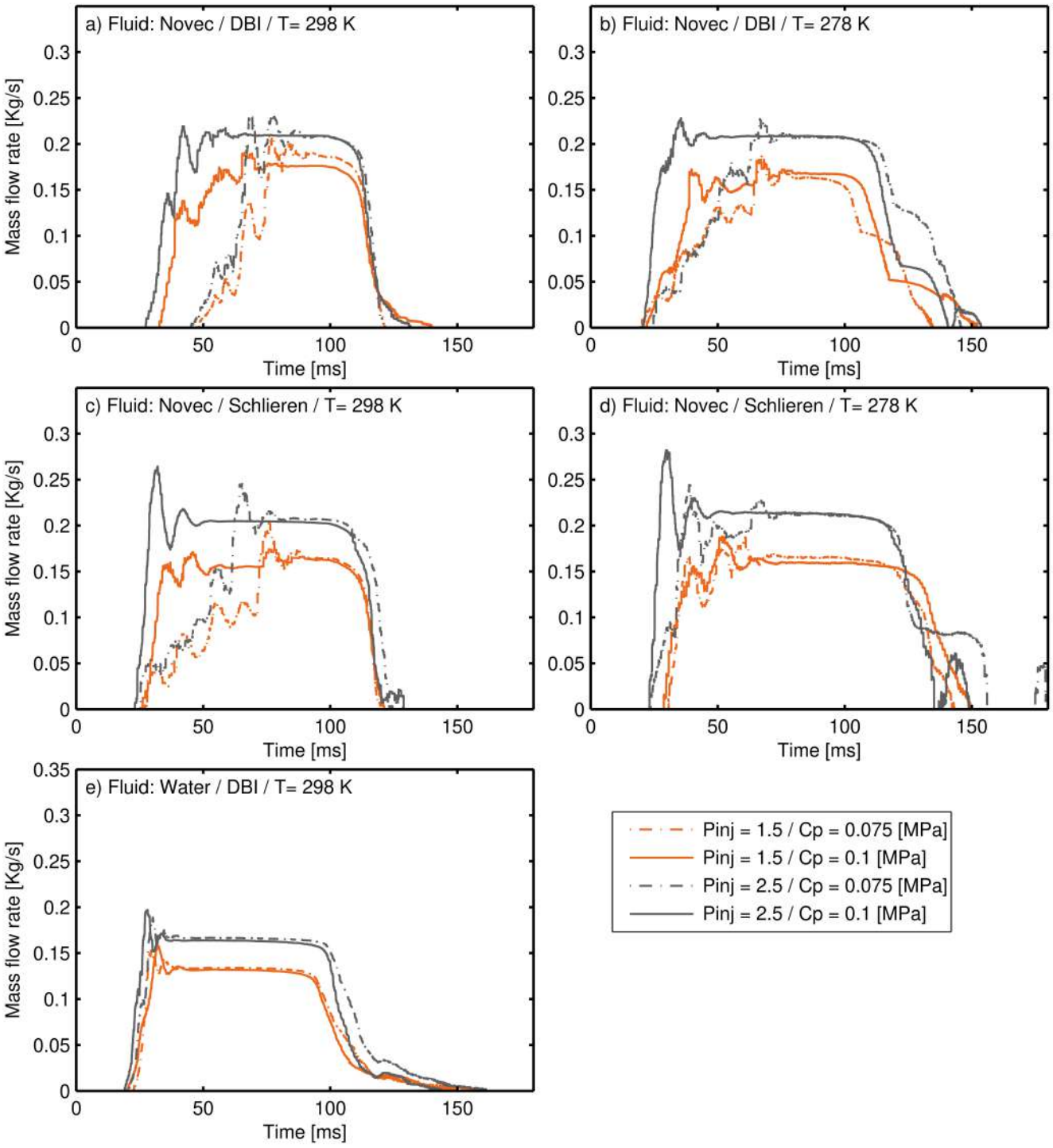

Figure 11: Time evolution of the mass flow rate during the suppressant injection event.

3.2. Spray penetration

Figure 12 shows a sample of the instantaneous spray development in the field of view #1 for the NewNozzle. These images are necessary to explain the singular behavior of the spray penetration curves at the first moments of the injection event. From the beginning of the injection to approximately 12 milliseconds there is a first liquid core corresponding to the liquid accumulated in the pipe which is pushed through the nozzle without the rotation momentum provided by the swirler of the nozzle producing a different behavior of the spray with no proper atomization, after that, the spray begins the atomization process and reaches the steady state. It can be seen how a second liquid core that is faster reaches the farthest zone of the spray.

This phenomenon was present in the beginning of all the measures taken induced by the presence of small amounts of liquid in the pipeline before each injection, however, it occurs at the first 15 milliseconds and it does not represent a problem in the performance of the fire extinguishing agent since if a fire occurs in the cargo cabin, the entire injection process would be in the order of magnitude of seconds, then for this work, only the steady-state (Figure 12e) is relevant.

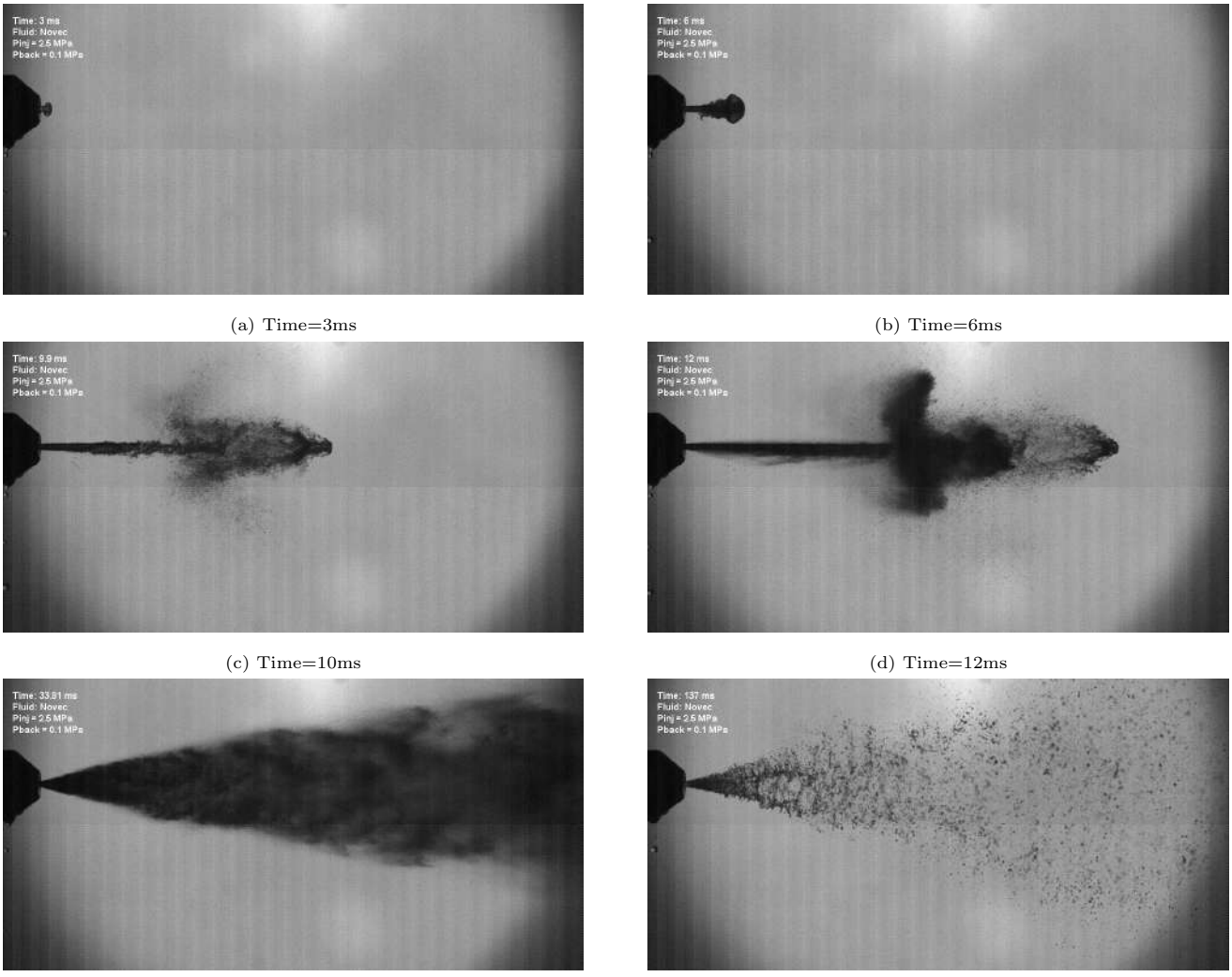

(a) Time=3ms

(b) Time=6ms

(c) Time=10ms

(d) Time=12ms

(e) Time=34ms (steady state)

(f) Time=137ms (end of injection)

Figure 12: Frame to frame samples of the injection event for Novec 1230.

Figure 13 shows the entire spray penetration development for water for the NewNozzle along all the fields of views, the red box indicates the field of view near to the nozzle exit and it is highlighted only because that position is taken into account to analyze the effects injection conditions in the spray penetration curves. It can be noticed that higher injection pressure leads to faster spray

penetration [34]. The shape of the curve changes from a parabolic trend to a straight line because in the first moments of the injection process the spray accelerates as it is injected. Afterward the spray reaches the steady state in which the pressure stabilizes and the spray speed is constant [35].

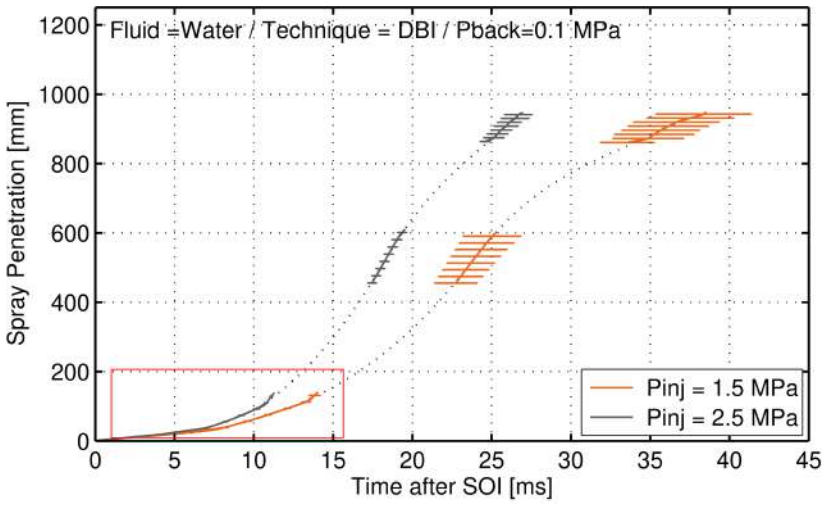

Figure 13: Water spray penetration along all the fields of views tested.

In Figures 14 and 15 it is observed that points at a higher temperature (298 K) and low back-pressure (0.075 MPa) have a differences in mass flow rate at the first moments of the injection events due to the fluid evaporation and the amount of liquid inside the pipe between the valves and the outlet of the nozzle. That phenomenon affects the spray penetration curves because at the beginning there is a mixture between the vapor and liquid phase of the injected fluid. This is a big issue in the spray contour detection because the stabilization of the injection occurs when the spray almost reaches the end of the visualization window of the first field of view and that is the reason why in almost all the penetration curves there is a fast change in the slope at the end. Although the spray reaches the end of the visualization window the criteria for the spray cone angle calculating is still valid if the end of the window is taken as maximum spray penetration.

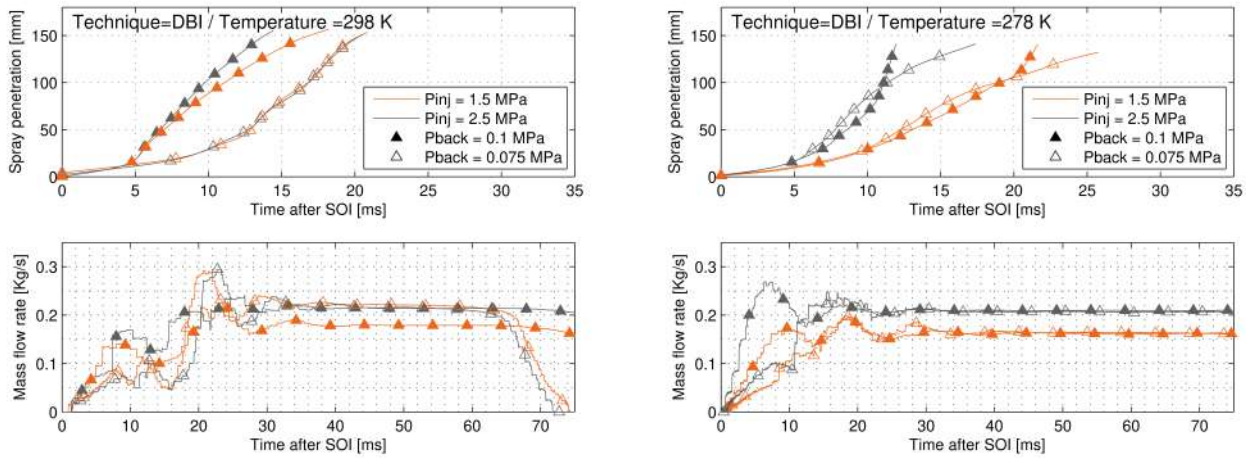

Figure 14: Penetration and mass flow rate comparison at different temperatures for FoV#1 and DBI technique for Novec1230.

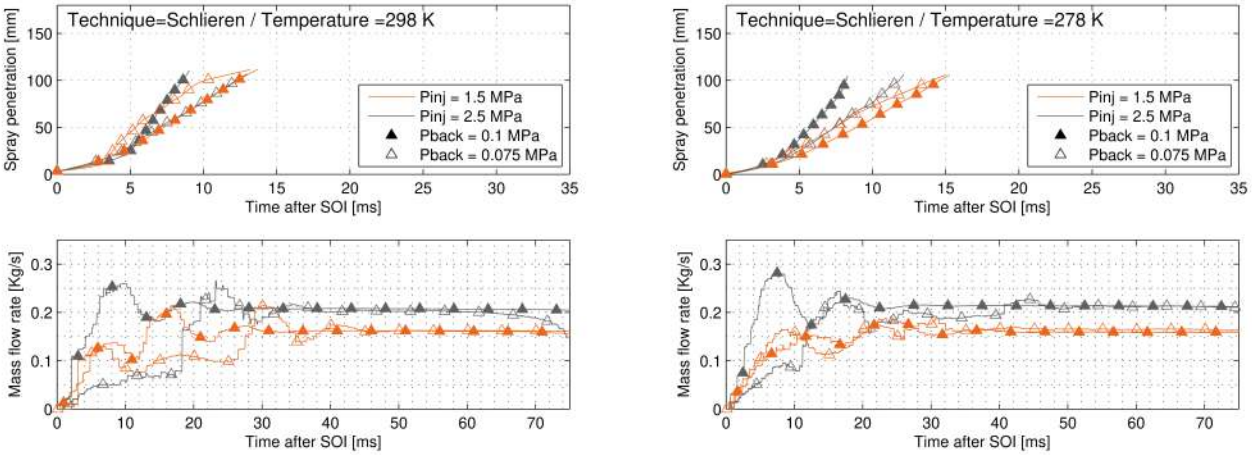

Figure 15: Penetration and mass flow rate comparison at different temperatures for FoV#1 and Schlieren technique for Novec1230.

As explained in 3.1 behavior in penetrations curves is related to fluid evaporation at first moments of the injection event that can be verified by the mass flow rate curves for each point.

3.3. Spray angle

Figure 16 shows the mean spray cone angle for different injection pressures, temperatures and back pressures. For this, only field of view #1 was analyzed.

It is observed that higher temperature and lower back-pressure induces a wider spray angle. The effect of the injection pressure on the spray angle is small and depends on the particular geometry of the nozzle [36]. For the case study an average spray angle of 25-30° was obtained for all conditions coinciding with what was reported by the manufacturer. The difference of 10-15% between the angle detected using the DBI and Schlieren techniques was produced by the detection of the vapor phase in the jet contour, as occurs when the evaporation process is significant during the injection event.

The standard deviation of the spray cone angles reported in Figure 16, taken in the steady state zone of the injection event, vary between 0.5° and 2.5°.

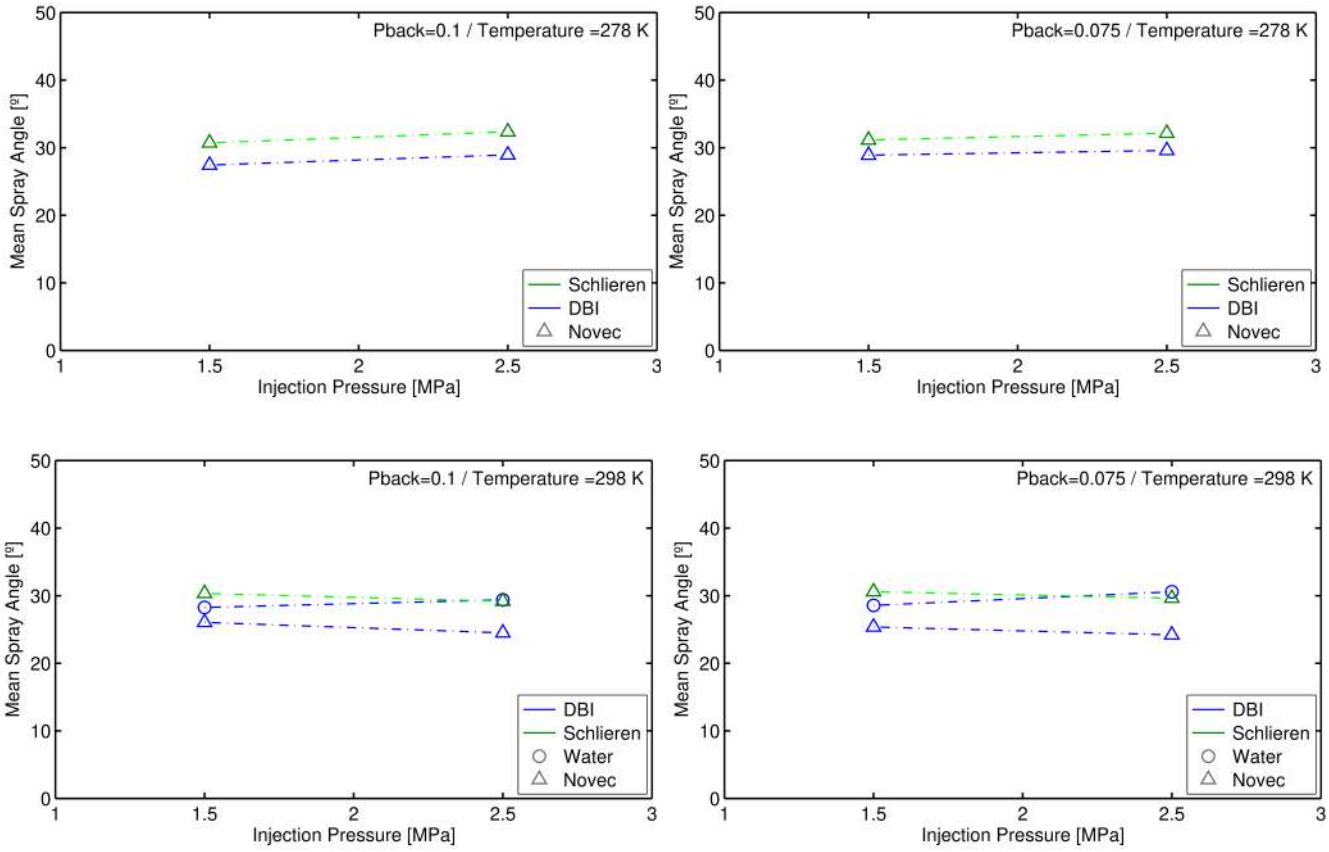

Figure 16: Averaged steady-state spray cone angle results for all the testing conditions.

3.4. Nozzles comparison

Both nozzles have the same outlet diameter the only difference is that the new nozzle has an internal piece that works as swirler that as said by Amini [37] induces the working fluid to pass under pressure through the tangential ports of the internal geometry of the nozzle to develop a free vortex in the swirl chamber of the nozzle. This rotational motion is intensified in the converging chamber while developing an axial flow component. Lastly, the fluid is ejected through the discharge orifice as a rotating tube.

Figure 17 shows the spray cone angle in the steady state zone of the injection

event, the bad performance of the old nozzle has been already reported [20]. The 30° of the spray angle of the new nozzle compared to the 0.5° of the old nozzle represents a huge improvement of the spray atomization and mixing, confirmed by the images acquired. These results ratify that the nozzles of the fire extinguisher system currently used in the aircraft cargo cabin do not work for these two alternative agents tested. Also, a higher spray angle means a wider spray at the furthest point of the test rig vessel that means a better distribution of the fire extinction agent in the airplane cargo cabin.

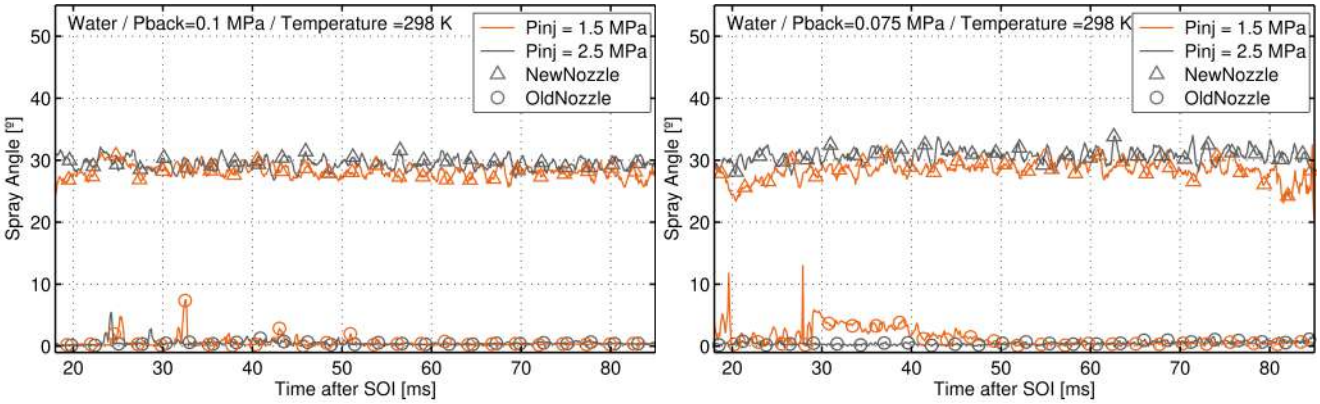

Figure 17: Steady state spray angle comparison between nozzles.

Figure 18 shows the spray penetration curves for the field of view #1 for both nozzles. As in the previous comparisons the conditions of the injection (injection pressure and back pressure) only produce slight variations on the spray behavior. Higher injection pressures leads to a faster spray penetration.

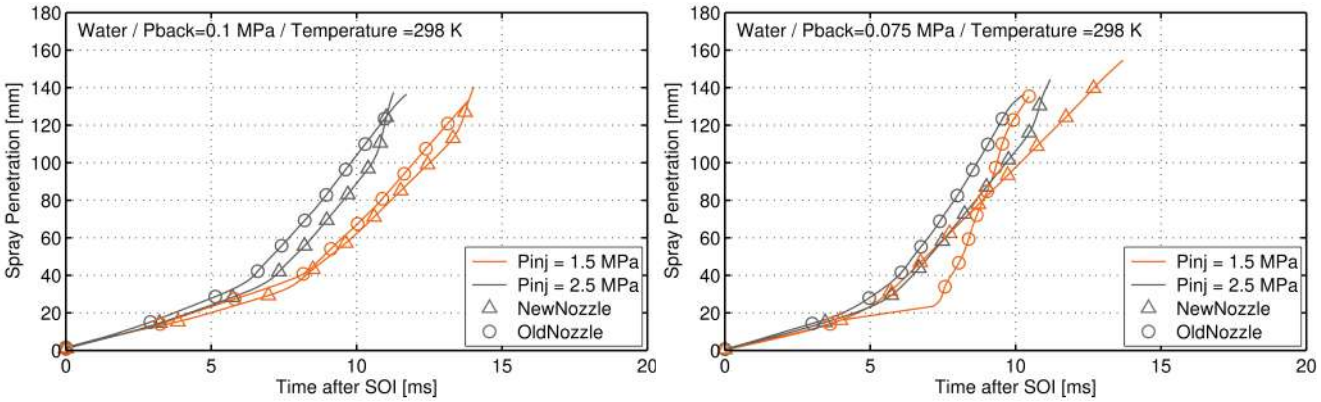

Figure 18: Spray penetration comparison between nozzles.

Figures 19 and 20 shows the frame to frame samples of the injection event of water for both nozzles. It can be seen a substantial difference in the spray cone angle for the NewNozzle at the steady state zone of the injection event 19d. In the case of the spray penetration the first moments of the injection event are similar until the internal swirler of the nozzle begins to take action.

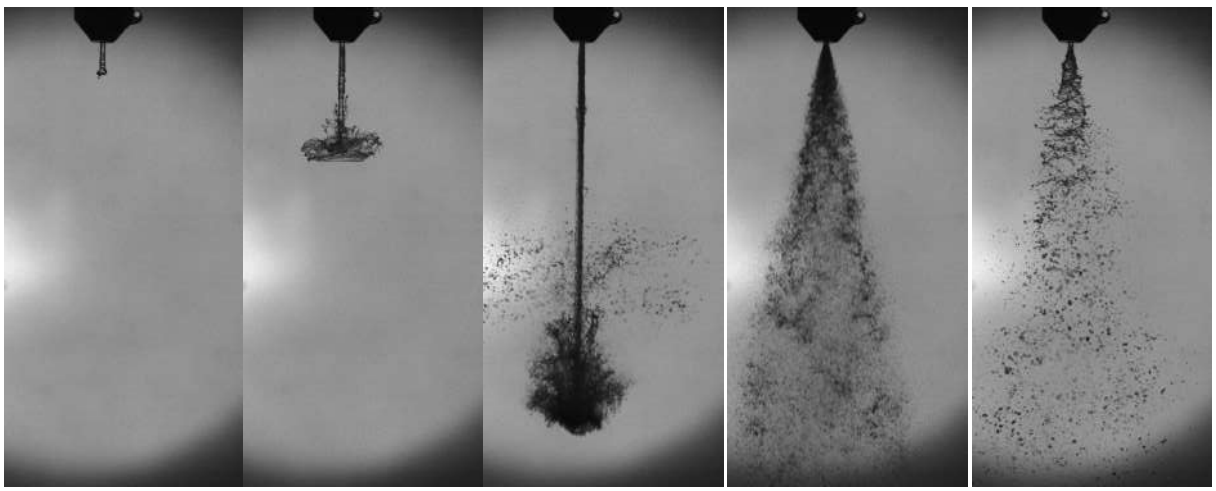

(a) Time=3ms (b) Time=8.54ms (c) Time=17.72ms (d) Time=48ms (steady state) (e) Time=115ms (end of injection)

Figure 19: Frame to frame samples of the injection event for water at 1.5 MPa and back pressure of 0.1 MPa with NewNozzle.

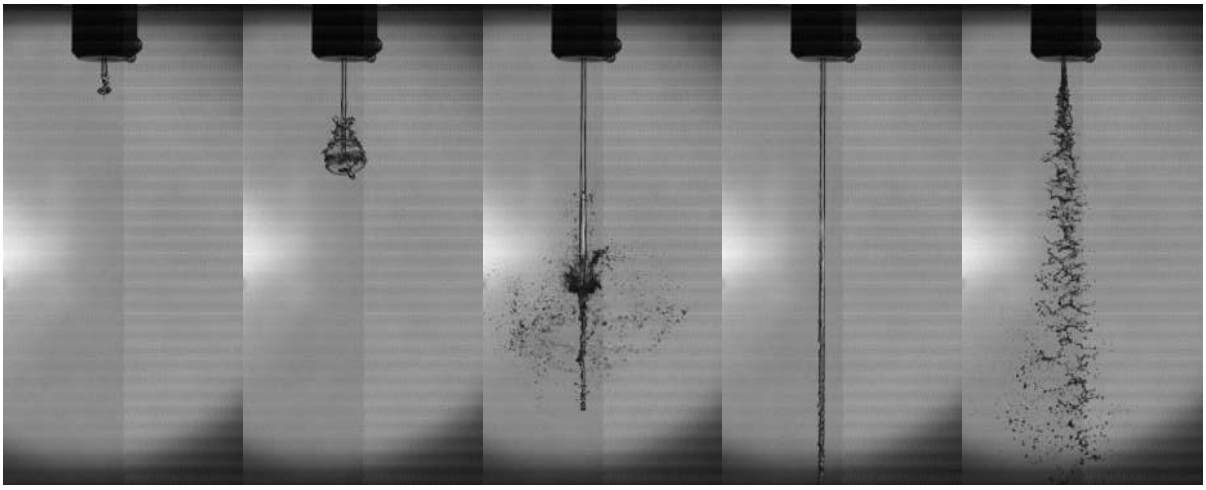

(a) Time=3ms (b) Time=8.54ms (c) Time=17.72ms (d) Time=48ms (steady state) (e) Time=115ms (end of injection)

Figure 20: Frame to frame samples of the injection event for water at 1.5 MPa and back pressure of 0.1 MPa with OldNozzle.

3.5. Alternative fire extinction agents images comparison

Figures [21-24] shows the images acquired with the high speed camera for the same injection pressure and back pressures for both nozzles, fluids and techniques used in the experimental campaign for all the field of views. Differences can be noticed between water and Novec1230 mostly at the beginning (close to the nozzle) and at the farthest point of the vessel. In the case of water there can be seen more liquid droplets in each FoV. The Schlieren technique 23 shows a huge amount of vapor phase in the FoV#3 which highlights the properties of Novec1230 as a possible substitute due to its good dispersion throughout the airplane cargo cabin together with its excellent properties as a fire extinguishing agent.

Figure 21: Example of the images acquired with the DBI technique for the NewNozzle with water at 2.5 MPa and back pressure of 0.1 Mpa.

Figure 22: Example of the images acquired with the DBI technique for the NewNozzle with Novec1230 at 2.5 MPa and back pressure of 0.1 Mpa.

Figure 23: Example of the images acquired with the Schlieren technique for the NewNozzle with Novec1230 at 2.5 MPa and back pressure of 0.1 Mpa.

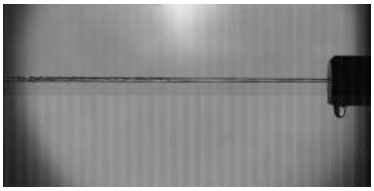

Figure 24: Example of the image acquired with the DBI technique for the OldNozzle with water at 2.5 MPa and back pressure of 0.1 Mpa.

Figure 24 shows the reason why the old nozzle (present in the fire extinguishing system of the airplanes cargo cabin) was changed in order to improve the spray atomization and enhance the agent distribution inside the test rig vessel because a small cone spray angle and a pure liquid jet was obtained.

4. Conclusions

A large constant pressure constant volume vessel was designed and assembled in order to test two new alternatives for replacing Halon 1301 in the fire suppression systems on aircraft cargo cabin. Macroscopic spray characteristics such as penetration and angle were obtained as a measure of the agent dispersion by the use of DBI and Schlieren optical techniques. At the same time, the mass flow rate of each injection event was calculated from the pressure signal upstream of the nozzle.

For the old nozzle and for the two fire extinctions agents tested (water and Novec 1230) most part of the spray was in liquid phase. Additionally, sprays have low atomization with opening angles between 0.5° and 5°. This implies poor agent distribution in the volume. Water injections do not show the presence of vapor phase, whilst some vapor Novec 1230 is found with the Schlieren technique around the liquid core jet. Even though, vapor presence is significant only for long distances far from the nozzle exit.

For the new nozzle whose geometry was selected in order to improve the spray atomization and to increase the cone spray angle as expected. The spray angle was increased to 30° which leads to a better atomization and distribution of the extinction agent inside the vessel. In the case of Novec 1230 huge amount of vapor phase was detected in the field of view #3 (the farthest point measured from the nozzle).

Spray penetration was measured for distances longer than 1m as a result of using three different fields of view along the spray axis inside the test rig. Due to its fluid properties, water penetrates into the volume faster than Novec 1230 although its mass flow rate through the orifice is lower. The expected trend when changing the injection pressure is found. The higher the injection pressure the faster the spray penetrates into the ambient. Temperature reduction tends to reduce the evaporation of Novec1230 slightly.

The effect of lower back-pressure is strongly even at the first moments of the spray development. The air/fire agent mix present in the pipe between

the valves and the nozzle outlet affects the shape of the mass flow rate at the beginning of the injection event. Also, the swirler of the new nozzle generates a new phenomenon at the beginning of the agent injection, where the first core of liquid injected do not have the tangential momentum induced by the internal geometry of the nozzle, this produce a three stages in the spray injection: first liquid core without tangential momentum (not relevant for the real application, where injection duration is in the order of seconds), second core under the swirler effects and the steady-state spray development.

Novec1230 has passed the FAA standards although with the current injection system its distribution in the airplane cargo cabin is inefficient. By changing the nozzle and maintaining the rest of the injection system it has been determined that the distribution of the agent improves, in addition to reducing the time needed for its change to the vapor phase.

Acknowledgments

This research was performed in the frame of the project "Multi-physics methodology for phase change due to rapidly depressurized two-phase flows" reference 785549 from Clean Sky Joint Undertaking. The authors would also like to thank José Enrique Del Rey for his help and participation in the test rig assembly as a lab technician.

References

[1] S. S. Hariram, Fire protection on airplanes, SAE Technical Papers (2005). doi:10.4271/2005-01-3429.

[2] R. G. Gann, Next-generation fire suppression technology program, Fire Technology 34 (1998) 363–371. doi:10.1023/A:1015370628661.

[3] J. L. Pagliaro, G. T. Linteris, Hydrocarbon flame inhibition by C6F12O (Novec 1230): Unstretched burning velocity measurements and predictions,

Fire Safety Journal 87 (2017) 10–17. doi:10.1016/j.firesaf.2016.11.002.

[4] J. Liu, G. Liao, P. Li, W. Fan, Q. Lu, Progress in research and application of water mist fire suppression technology, Chinese Science Bulletin 48 (2003) 718–725. doi:10.1360/02ww0180.

[5] C. Hipsher, D. Ferguson, Fire Protection: Cargo Compartments, Aero Magazine (2011).

[6] D. G. Elliott, P. W. Garrison, G. A. Klein, K. M. Moran, M. P. Zydowicz, Flow of nitrogen-pressurized Halon 1301 in fire extinguishing systems, JPL Publication 84-62 62 (1984) 1–124.

[7] N. ISO, ISO 14520-5. Gaseous fire-extinguishing systems - Physical properties and system design - 2016 (2016) 2–7.

[8] R. Maker, T. R., Sarkos, C. P., Hill, in: 88th Symp. of the propulsion and energetics panel on aircraft fire safety.

[9] P. Yang, T. Liu, X. Qin, Experimental and numerical study on water mist suppression system on room fire, Building and Environment 45 (2010) 2309–2316. doi:10.1016/j.buildenv.2010.04.017.

[10] S. C. Kim, H. S. Ryou, An experimental and numerical study on fire suppression using a water mist in an enclosure, Building and Environment 38 (2003) 1309–1316. doi:10.1016/S0360-1323(03)00134-3.

[11] M. gao YU, K. YANG, H. lin JIA, C. LU, L. xiang LU, Coal combustion restrained by ultra-fine water mist in confined space, Mining Science and Technology 19 (2009) 574–579. doi:10.1016/S1674-5264(09)60107-1.

[12] C. W. Chiu, Y. H. Li, Full-scale experimental and numerical analysis of water mist system for sheltered fire sources in wind generator compartment, Process Safety and Environmental Protection 98 (2015) 40–49. doi:10.1016/j.psep.2015.05.011.

[13] Z. Liu, A. Kim, A review of water mist fire suppression systems - fundamental studies, Journal of Fire Protection Engineering 1 (1999) 20. doi:10.1177/104239158900100101.

[14] R. Wighus, Extinguishment of Enclosed Gas Fires with Water Spray, Fire safety science-proceedings of the third international symposium. (2007) 997–1006.

[15] C. C. Ndubizu, R. Ananth, P. A. Tatem, Effects of droplet size and injection orientation on water mist suppression of low and high boiling point liquid pool fires, Combustion science and technology 157 (2000) 63–86. doi:10.1080/00102200008947310.

[16] K. Prasad, C. Li, K. Kailasanath, Simulation of water mist suppression of small scale methanol liquid pool fires, Fire Safety Journal 33 (1999) 185–212. doi:10.1016/S0379-7112(99)00028-4.

[17] A. U. Modak, A. Abbud-Madrid, J. P. Delplanque, R. J. Kee, The effect of mono-dispersed water mist on the suppression of laminar premixed hydrogen-, methane-, and propane-air flames, Combustion and Flame 144 (2006) 103–111. doi:10.1016/j.combustflame.2005.07.003.

[18] L. Yinshui, J. Zhuo, W. Dan, L. Xiaohui, Experimental research on the water mist fire suppression performance in an enclosed space by changing the characteristics of nozzles, Experimental Thermal and Fluid Science 52 (2014) 174–181. doi:10.1016/j.expthermflusci.2013.09.008.

[19] T. Liang, M. Liu, Z. Liu, W. Zhong, X. Xiao, S. Lo, A study of the probability distribution of pool fire extinguishing times using water mist, Process Safety and Environmental Protection 93 (2015) 240–248. doi:10.1016/j.psep.2014.05.009.

[20] R. Payri, J. Gimeno, P. Martí-aldaraví, C. Carvallo, Experimental study of the dispersion of a fire suppression agent through a real size nozzle of an aircraft cargo cabin extinguisher system (2019) 2–4.

[21] W. Grosshandler, C. Presser, D. Lowe, W. Rinkinen, Assessing halon alternatives for aircraft engine nacelle fire suppression, Journal of Heat Transfer 117 (1995) 489–494. doi:10.1115/1.2822548.

[22] M. O. McLinden, R. A. Perkins, E. W. Lemmon, T. J. Fortin, Thermodynamic properties of 1,1,1,2,2,4,5,5,5-nonafluoro-4-(trifluoromethyl)-3-pentanone: Vapor pressure, (p, ρ, T) behavior, and speed of sound measurements, and an equation of state, Journal of Chemical and Engineering Data 60 (2015) 3646–3659. doi:10.1021/acs.jced.5b00623.

[23] R. D. Reitz, F. V. Bracco, Mechanism of atomization of a liquid jet, Physics of Fluids 25 (1982) 1730–1742. doi:10.1063/1.863650.

[24] ECN, ECN, Engine Combustion Network, 2015. URL: www.sandia.gov/ecn/.

[25] G. S. Settles, Schlieren and Shadowgraph Techniques, 2001. doi:10.1007/978-3-642-56640-0.

[26] J. V. Pastor, R. Payri, J. M. Garcia-Oliver, J.-G. Nerva, Schlieren Measurements of the ECN-Spray A Penetration under Inert and Reacting Conditions, SAE Technical Paper 2012-01-0456 (2012). doi:10.4271/2012-01-0456.

[27] R. Payri, J. M. Garcia-Oliver, M. Bardi, J. Manin, Fuel temperature influence on diesel sprays in inert and reacting conditions, Applied Thermal Engineering 35 (2012) 185–195. doi:10.1016/j.applthermaleng.2011.10.027.

[28] C. Gong, M. Jangi, X. S. Bai, Large eddy simulation of n-Dodecane spray combustion in a high pressure combustion vessel, Applied Energy 136 (2014) 373–381. doi:10.1016/j.apenergy.2014.09.030.

[29] C. L. Genzale, R. D. Reitz, M. P. B. Musculus, Effects of spray targeting on mixture development and emissions formation in late-injection low-

temperature heavy-duty diesel combustion, Proceedings of the Combustion Institute 32 II (2009) 2767–2774. doi:10.1016/j.proci.2008.06.072.

[30] L. M. Pickett, C. L. Genzale, J. Manin, L.-M. Malbec, Measurement Uncertainty of Liquid Penetration in Evaporating Diesel Sprays, Most (2011).

[31] H. Chaves, M. Knapp, A. Kubitzek, F. Obermeier, T. Schneider, Experimental study of cavitation in the nozzle hole of diesel injectors using transparent nozzles, SAE Technical Papers (1995). doi:10.4271/950290.

[32] D. L. Siebers, Scaling liquid-phase fuel penetration in diesel sprays based on mixing-limited vaporization, SAE Technical Papers (1999). doi:10.4271/1999-01-0528.

[33] E. A.Lichtarowicz,R.K Duggins, Separation Cavitation in Lightly Loaded Fluid (1974). doi:10.1243/JMES.

[34] R. Payri, F. J. Salvador, G. Bracho, A. Viera, Differences between single and double-pass schlieren imaging on diesel vapor spray characteristics, Applied Thermal Engineering 125 (2017) 220–231. doi:10.1016/j.applthermaleng.2017.06.140.

[35] P. G. Aleiferis, Z. R. Van Romunde, An analysis of spray development with iso-octane, n-pentane, gasoline, ethanol and n-butanol from a multi-hole injector under hot fuel conditions, Fuel 105 (2013) 143–168. doi:10.1016/j.fuel.2012.07.044.

[36] F. Payri, R. Payri, M. Bardi, M. Carreres, Engine combustion network: Influence of the gas properties on the spray penetration and spreading angle, Experimental Thermal and Fluid Science 53 (2014) 236–243. doi:10.1016/j.expthermflusci.2013.12.014.

[37] G. Amini, Liquid flow in a simplex swirl nozzle, International Journal of Multiphase Flow 79 (2016) 225–235. doi:10.1016/j.ijmultiphaseflow.2015.09.004.